The Global Distribution and Drivers of Grazing Dynamics Estimated from Inverse Modelling

Tyler Rohr[1,2], Anthony Richardson[3,4], Andrew Lenton[5], Matt Chamberlain[5], Elizabeth Shadwick[2,5]

[2]Institute for Marine and Antarctic Science, University of Tasmania, Hobart, Tasmania, 7000, Australia
[2]Australian Antarctic Partnership Program, Hobart, Tasmania, 7000, Australia
[3]School of Environment, The University of Queensland, St Lucia, 4072, Queensland, Australia
[4]Commonwealth Scientific and Industrial Research Organisation (CSIRO) Environment, BioSciences Precinct (QBP), St Lucia, Queensland, 4067, Australia
[5]Commonwealth Scientific and Industrial Research Organisation (CSIRO) Environment, Hobart, Tasmania, 7000 Australia

Key Points:

- Oligotrophic (eutrophic) biomes exhibit more (less) efficient community-integrated grazing, characteristic of micro- (meso-) zooplankton.
- We find a strong link between observed mean-annual phytoplankton biomass and the grazing dynamics required to recreate its seasonal cycle.
- A type III functional response does a consistently better job recreating observed phytoplankton seasonal cycles than a type II response.

Corresponding author: Tyler Rohr, `tyler.rohr@utas.edu.au`

Abstract

We use inverse modelling to infer the distribution and drivers of community-integrated zooplankton grazing dynamics based on the skill with which different grazing formulations recreate the satellite-observed seasonal cycle in phytoplankton biomass. We find that oligotrophic and eutrophic biomes require more and less efficient grazing dynamics, respectively. This is characteristic of micro- and mesozooplankton, respectively, and leads to a strong sigmoidal relationship between observed mean-annual phytoplankton biomass and the optimal grazing parameterization required to simulate its seasonal cycle. Globally, we find type III rather than type II functional response curves consistently exhibit higher skill. These new observationally-based distributions can help constrain, validate and develop next-generation biogeochemical models.

Plain Language Summary

To improve predictions of our ocean's ability to feed a growing human population and buffer a changing climate, we need to improve our understanding of what happens to carbon once it is absorbed into the ocean. One of the largest gaps in marine carbon cycling is the role of zooplankton grazing. The rate at which zooplankton graze phytoplankton modifies the size and seasonal evolution of phytoplankton populations and in turn the associated rates of net primary production at the base of the food web, secondary production of grazers (an indicator of fisheries potential) and export production (the biological sequestration of carbon). However, regional differences in grazing, which are difficult to measure outside of a laboratory setting, remain poorly constrained by observations and thus difficult to model. Here, we run a suite of model simulations, each of which simulate grazing in a different way, then compare the results to infer which type of grazing dynamics match observations. We find that there is dramatic spatial variability in how zooplankton, as a community, appear to be grazing and that this variability maps well onto observed phytoplankton concentrations, suggesting that the type of zooplankton present may be determined by the amount of prey available.

1 Introduction

Marine net primary production (NPP) supports the biological export (EP) of carbon (de la Rocha, 2006) and forms the base of the marine food web (Armengol et al., 2019). Although oceanographers have historically focused on light (Sverdrup, 1953) and nutrients (Howarth, 1988), increasing experimental (Lima-Mendez et al., 2015; Guidi et al., 2016), observational (Behrenfeld et al., 2013) and modelling (Hashioka et al., 2013; Prowe et al., 2012; Laufkötter et al., 2015; Vallina & Le Quéré, 2011; Chenillat et al., 2021) work has highlighted zooplankton grazing as a critical control on NPP. However, grazing dynamics remain poorly constrained across modern biogeochemical (BGC) models, including those used by the IPCC in climate projections (Rohr et al., 2023). This likely contributes to persisting uncertainty in projections of NPP (Tagliabue et al., 2021; Laufkötter et al., 2015), EP (Laufkötter et al., 2016; Fu et al., 2016), zooplankton biomass (Petrik et al., 2022) and fisheries catch (Tittensor et al., 2021).

The parameterization of relatively coarse global models implicitly requires an understanding of the mean dynamics of many species averaged across a patchy ocean, which may diverge dramatically from the dynamics of individual zooplankton (Rohr et al., 2022; Morozov, 2010). Although empirical laboratory experiments have shown that grazing dynamics (i.e. the manner in which zooplankton-specific grazing rates increase with prey concentration) vary substantially across zooplankton species, ages, and sizes (Hansen et al., 1997; Hirst & Bunker, 2003), most laboratory studies consider the idealized behavior of a single species in a well-mixed environment.

Field-based dilution experiments help average across some of this variability (Morrow et al., 2018; Landry et al., 2009, 2008; Landry et al., 2000) and have been used to estimate grazing dynamics in natural microzooplankton assemblages (Chen et al., 2014). However, these experiments are limited in their spatial scope and resolution (Schmoker et al., 2013) and can be biased by trophic cascades (Calbet et al., 2011), the presence of mixotrophs (Calbet et al., 2012) and the exclusion of mesozooplankton and macrozooplankton (Schmoker et al., 2013).

In the absence of direct, global, high-resolution measurements, community-integrated grazing rates and dynamics could theoretically be backed-out from zooplankton biomass budgets. However, disparate methods for shipboard observation make it difficult to describe time-evolving global distributions without large levels of statistical inference (Everett et al., 2017; Heneghan et al., 2020; Ratnarajah et al., 2023) and algorithms for satellite observation are limited (Druon et al., 2019; Strömberg et al., 2009).

Yet, while zooplankton grazing dynamics and biomass are difficult to observe directly, phytoplankton loss rates (Mojica et al., 2021; Deppeler & Davidson, 2017) and population dynamics (Gentleman & Neuheimer, 2008; Truscott et al., 1994; Steele, 1974) are largely driven by grazing. Thus the most viable option to estimate community-integrated grazing dynamics at scale may be inference from the remote sensing record of phytoplankton biomass (Westberry et al., 2008).

Here, we infer the global distribution of community-integrated grazing dynamics using an inverse modelling approach. We run a suite of simulations in a coupled ocean-BGC model, parameterized with a wide range of grazing dynamics, and determine the optimal parameters required to recreate the observed phytoplankton seasonal cycle. We map the distribution of optimal parameters, examine how they appear driven by regional variability in phytoplankton biomass (**Sec. 3.1**), and explain mechanistically how grazing dynamics can shape the seasonal cycle (**Sec. 3.2**). Finally, we discuss the limitations of this work (**Sec. 4.1**), as well its potential utility from a ecological (**Sec. 4.2**) and modelling perspective (**Sec. 4.3**).

2 Materials and methods

2.1 Grazing in BGC models

The simplest BGC models include one zooplankton grazing on one phytoplankton. The relationship between specific grazing rates (g; d^{-1}) and prey abundance is typically described by a type II or III functional response curve (Gentleman & Neuheimer, 2008; Rohr et al., 2022). The primary difference between response curves is that the type II response increases linearly at low phytoplantkon concentrations ($[C_{phyto}]$; mmolC m^{-3}), while the type III increases quadratically (**Figure 1**). Both curves, $g([C_{phyto}])$, can be parameterized with a saturation grazing rate (g_{max}; d^{-1}), which describes the rate when prey is non-limiting, and a half saturation concentration ($K_{1/2}$; mmolC m^{-3}), which describes how much prey is required to get there (i.e. $g([K_{1/2}]) = 0.5 * g_{max}$). Here we focus on $K_{1/2}$ because it has been shown to have a stronger influence on population dynamics (Rohr et al., 2022) and marine carbon cycling (Rohr et al., 2023) than g_{max}.

2.2 Grazing and population dynamics

Grazing dynamics can influence the seasonal cycle of phytoplankton biomass via the curvature of the functional response, which has either a stabilizing or destabilising influence on phytoplankton population dynamics depending on its concavity (Steele, 1974; Truscott et al., 1994; Gentleman & Neuheimer, 2008; Rohr et al., 2022). If the functional response is concave upward, then phytoplankton-specific loss rates to grazing increase with the size of the phytoplankton population. This creates a negative feedback loop which

dampens changes in the size of the phytoplankton population, thereby exerting a stabilizing influence. Alternatively, downward concavity means phytoplankton-specific loss rates to grazing decline with population growth, creating a destabilizing, positive feedback which amplifies changes in the size of the phytoplankton population.

The shape and stabilizing influence of the functional response is determined by its response type (II or III) and parameters (particularly $K_{1/2}$). While the parameter values determine the magnitude of curvature and thus the strength of the stabilizing influence, the response type determines the direction. A type II response is always concave downward and thus always destabilizing. A type III response has upward concavity below $K_{1/2}$ and thus stabilizing properties at low phytoplankton concentrations. In turn, the grazing formulation exerts a strong influence on the size, shape, and propensity of phytoplankton blooms, sub-seasonal oscillations, and extinction events (Dunn & Hovel, 2020; Adjou et al., 2012; Hernández-García & López, 2004; Malchow et al., 2005; Rohr et al., 2022).

While a type II response is typically found in laboratory experiments (Hansen et al., 1997), a type III response can be justified as the implicit representation of more complex behavior such as active prey switching (Prowe et al., 2012; Vallina et al., 2014) or the mean state of a patchy ocean (Morozov & Arashkevich, 2010; Rohr et al., 2022). Thus, in any given region, the true shape of the apparent functional response (i.e. the spatially-integrated relationship between total prey and community-averaged zooplankton-specific grazing rates) is determined by the community-composition, prey preferences, spatial distributions and physiology of resident zooplankton. Using inverse modelling to match the spatially-averaged and community-integrated phytoplankton record observed from satellites helps average out spatial, species-level, and behavioral complexities that many global models do not explicitly resolve.

2.3 Model configuration

We use a global, ocean-BGC model to determine which $K_{1/2}$ values and response types are required to best match the observed phytoplankton seasonal cycle. Simulations are run with the Whole Ocean Model of Biogeochemistry and Trophic-dynamics (WOMBAT) (Law et al., 2017), part of the Australian Earth Systems Model (ACCESS-ESM1.5) (Ziehn et al., 2020), which has been studied and validated extensively (Mortenson et al., 2021; Kwiatkowski et al., 2020; Ziehn et al., 2017; Oke et al., 2013). The ocean model is the global configuration of Modular Ocean Model version 5 (Griffies, 2012). WOMBAT has a relatively simple structure, with one phytoplankton and one zooplankton group. While more complex models include multiple zooplankton grazing on multiple phytoplankton (Rohr et al., 2023), we are interested here in estimating community-integrated grazing dynamics. These can be inferred most directly by tuning WOMBAT's single-prey grazing formulation, which implicitly represents the community-integrated behavior of all zooplankton groups, towards the satellite-observed phytoplankton seasonal cycle, which explicitly integrates across all phytoplankton groups.

2.4 Model experiments

We ran a total of 36 global simulations, each with a different grazing formulation. To isolate the influence of grazing, all simulations were initialized from the same state, embedded in an identical repeat-climatological physical ocean, and forced with identical surface flux and freshwater runoff from the Japanese 55-year atmospheric reanalysis surface dataset (Tsujino et al., 2020). After initialisation, each run was spun up for 5 years to a quasi-steady state, long enough to equilibrate with changes to the grazing formulation. Output is reported from the fifth year and can be considered climatological.

We ran two suites of experiments, using a type II and III functional response. Within each suite, we tested 18 different parameters combination: $K_{1/2} = 0.5,\ 1,\ 2,\ 4,\ 8,\ 16$ $(mmolC\ m^{-3})$ and $g_{max} = 0.5,\ 1,\ 2\ (d^{-1})$. These values are consistent with the range that has been derived empirically and used in models historically (Rohr et al., 2022). All other parameters were kept constant and identical to Law et al. (2017).

2.5 Model skill assessment

We used two metrics to evaluate the model's ability to recreate the observed phytoplankton seasonal cycle: the correlation coefficient (CC) and the coefficient of variation (CV). The CC measures the co-variability between the simulated and observed climatologies, while the CV measures the magnitude of variability separately in each climatology relative to its annual mean ($CV = \frac{std}{mean}$). Together they capture the shape (CC) and strength (CV) of the seasonal cycle. Both metrics are largely agnostic to the size of mean-annual phytoplankton population (i.e. CC independent to mean; CV normalized by mean). This is to help isolate the influence of grazing dynamics on the qualitative shape of the seasonal cycle rather than mean-state NPP which could be biased by many other model attributes.

For each metric, the seasonal cycle of simulated surface phytoplankton biomass was compared to an 18-year remote sensing climatology (July 2002 - April 2021) from the Carbon-based Productivity Model (CbPM) (Westberry et al., 2008). The remote sensing record was interpolated onto the model grid and all time series were centered on the summer solstice. We use the observed carbon product, which is derived from back-scatter, instead chlorophyll because WOMBAT does not resolve chlorophyll. However, we repeated the analysis comparing model carbon to satellite chlorophyll (Sathyendranath et al., 2019) and found similar results (**Supporting Text 1**).

The cost function for model skill was quantified for each run in each grid-cell by subtracting the absolute difference between the modelled (CV_{mod}) and observed (CV_{obs}) coefficient of variation from the correlation coefficient ($CC_{mod,obs}$),

$$\text{Model Skill} = norm(CC_{mod,obs}) - norm(|CV_{mod} - CV_{obs}|) \tag{1}$$

Both metrics are normalized across all grid cells from all 36 model runs, such that they are equally weighted and cost function scores can be directly compared across all experiments.

For each response type, we considered three sets of six runs. Each run in a set used a different $K_{1/2}$ value but constant g_{max} value. Within each set, the cost function score was interpolated between $K_{1/2}$ values at each grid cell using a piece-wise cubic polynomial (**Figure 2**). The $K_{1/2}$ value with the maximum score was identified and averaged across all three sets to infer the optimal value. Regions below 55°S or above 55°N with limited remote sensing coverage were excluded.

3 Results

3.1 Global distribution and drivers of grazing dynamics

The distribution of observed mean-annual surface phytoplankton biomass estimated from CbPM (**Figure 1A**) has a striking co-variability with the distribution of grazing dynamics inferred by the optimal $K_{1/2}$ value required to match the observed seasonal cycle (**Figure 1B, C**). We find that more oligotrophic regions with mean-annual phytoplankton biomass lower than the global median require smaller $K_{1/2}$ values to best match the observed phenology (**Figure 1A-C; more blue**). Alternatively, eutrophic regions with mean-annual phytoplankton biomass above the global median, including HNLC re-

gions, require larger $K_{1/2}$ values (**Figure 1A-C; more green**). Qualitatively, this pattern generally holds regardless of whether a type II (**Figure 1B**) or III (**Figure 1C**) functional response is used to described grazing dynamics and whether biomass (**Figure 1A**) or chlorophyll (**Supporting Figure 1**) is used to described the observed seasonal cycle.

Plotting the optimal $K_{1/2}$ value against the corresponding observed mean-annual surface biomass reveals a clear sigmoidal relationship (**Figure 1D, E**). Regardless of functional response type, larger $K_{1/2}$ values are required to recreate the seasonal cycle of biomes with higher mean-annual phytoplankton biomass, but appear to be bound asymptotically by a minimum and maximum viable $K_{1/2}$ value. Switching from a type II (**Figure 1D**) to type III (**Figure 1E**) response or decreasing g_{max} (**Supporting Figure 2**) decreases the value of both asymptotes, but neither substantively influence the shape of the curve. Thus, while other assumptions about the grazing formulation influence the specific quantitative estimates of the optimal $K_{1/2}$ (**Supporting Table 1**), the qualitative relationship is consistent: higher biomass regions appear to be populated with zooplankton with higher community-integrated $K_{1/2}$ values.

Finally, regardless of biome, using a type III response consistently recreates the observed phytoplankton seasonal cycle better than a type II response, with 30% more model skill on average (**Figure 1**). Moreover, the type III response performs better regardless of whether the observed seasonal cycle is quantified with carbon or chlorophyll or which g_{max} value is used (**Supporting Figures 1, 2**).

3.2 Mechanistic influence of the grazing dynamics

Importantly, our estimations of model skill do not include any metric for mean model bias. Thus, the correct interpretation of these results is not that more or less grazing leads to less or more phytoplankton biomass, respectively, but rather that the dynamical properties of the functional response curve can shape of the seasonal evolution of phytoplankton accumulation in a way that appears more or less consistent with observations.

For example, when $K_{1/2}$ is large, phytoplankton tend to exhibit a stronger, well-defined seasonal cycle with less high frequency variability (**Figure 2**; green lines). This is because the grazing formulation does not heavily influence the stability of the system, allowing bloom dynamics to be driven primarily by bottom-up controls, such as light and nutrients, which generally exhibit strong seasonality following seasonal cycles in vertical mixing and day length. In turn, phytoplankton population dynamics are not as sensitive to the whether a type II (**Figure 2C, D**) or III (**Figure 2A, B**) response is used. However, as $K_{1/2}$ decreases, the grazing formulation has a stronger influence on the stability on the system. This influence is stabilizing if a type III response is used but destabilizing if a type II response is used (**Supporting Text 2; Supporting Figure 3**), resulting in substantively different seasonal cycles (**Figure 2**; blue tracers). We consider two case studies, in the Subantarctic zone (SAZ) and Sargasso sea, which are generally representative of the seasonal variability in more eutrophic and oligotrophic biomes, respectively.

In the SAZ (**Figure 2A, C**) the observed evolution of biomass (black line) exhibits a strong seasonal cycle with an amplitude $\sim 20\%$ greater than its mean and relatively little sub-seasonal variability. It is best recreated using larger $K_{1/2}$ values and exhibits slightly more model skill when a type III response is used. With a type III response (**Figure 2A**), lower $K_{1/2}$ values reduce the mean biomass but do not systematically modify the CV, leaving the ratio of summer to winter biomass roughly proportional. Alternatively, with a type II response (**Figure 2C**), decreasing $K_{1/2}$ delays bloom initiation but amplifies its acceleration once initiated, leading to smaller, shorter, sharper features and systematically higher CVs. The initiation is delayed because the type II response disproportionately increases grazing rates at low biomass concentrations compared to a type

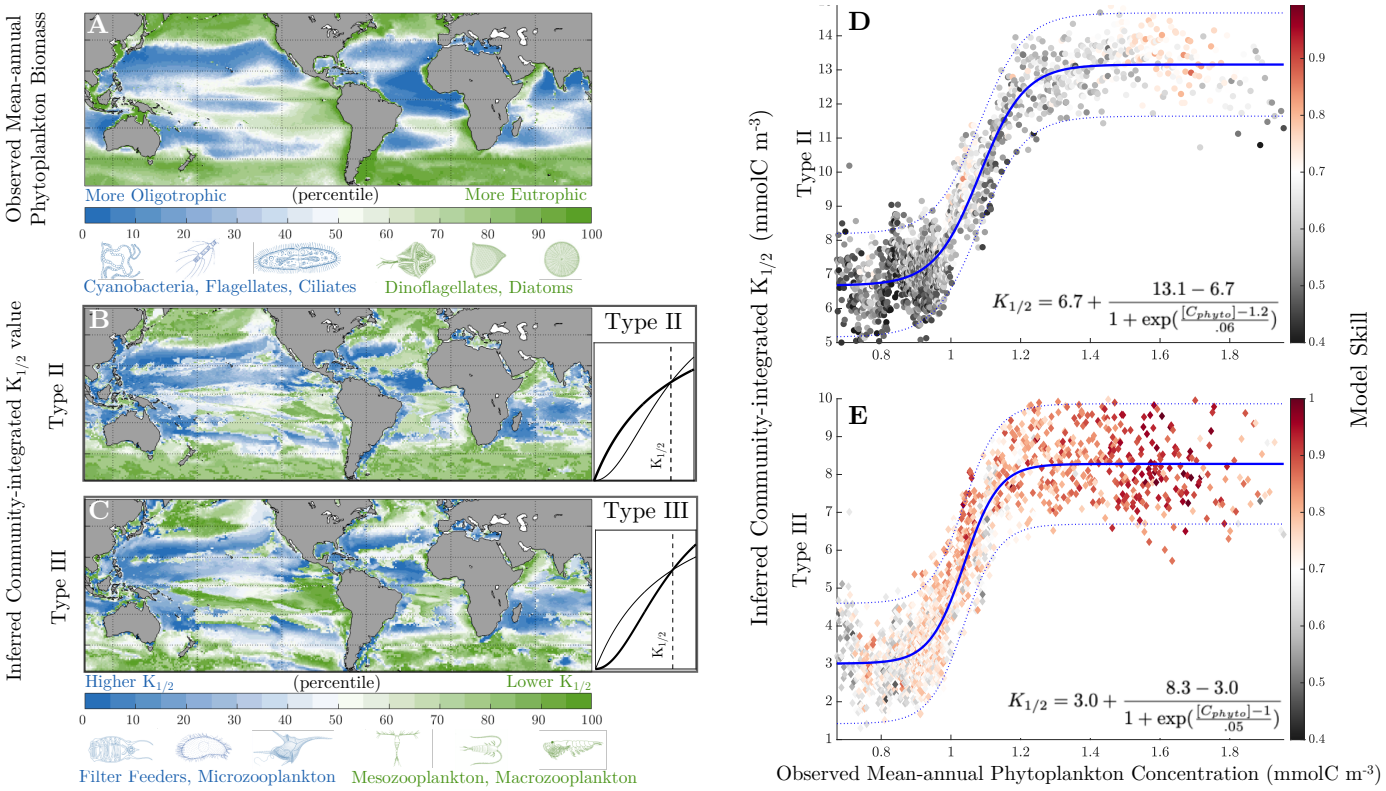

Figure 1. The distribution and drivers of grazing dynamics. **A)** The observed climatological mean-annual phytoplankton biomass concentration plotted as a percentile of the full spatial distribution. Below, the corresponding optimal $K_{1/2}$ parameter required to best recreate the observed phytoplankton seasonal cycle using a **B)** type II or **C)** type III response function plotted as a percentile for direct qualitative comparison. Beside each is an example functional response curve for their respective (bolded) response types, both parameterized with the same $K_{1/2}$ and g_{max}. Below **A)** a schematic of the characteristic phytoplankton associated with low and high biomass waters and below **C)** a schematic of zooplankton associated with low and high $K_{1/2}$ values. The optimal $K_{1/2}$ found with a **D)** type II and **E)** type III response are plotted against the observed mean-annual phytoplankton biomass. Each point represents the mean of roughly 30 grid cells, binned based on their percentile biomass, with the top and bottom 5% percent removed. Points are colored by their mean cost function score, with red indicating more model skill. All values are averaged across three experiment suites, with each using a different g_{max} value. Results from individual experiment suites are shown in **Supporting Figure 2**. Data is fit to a sigmoidal curve (solid blue), shown with 95% confidence bounds (dashed blue).

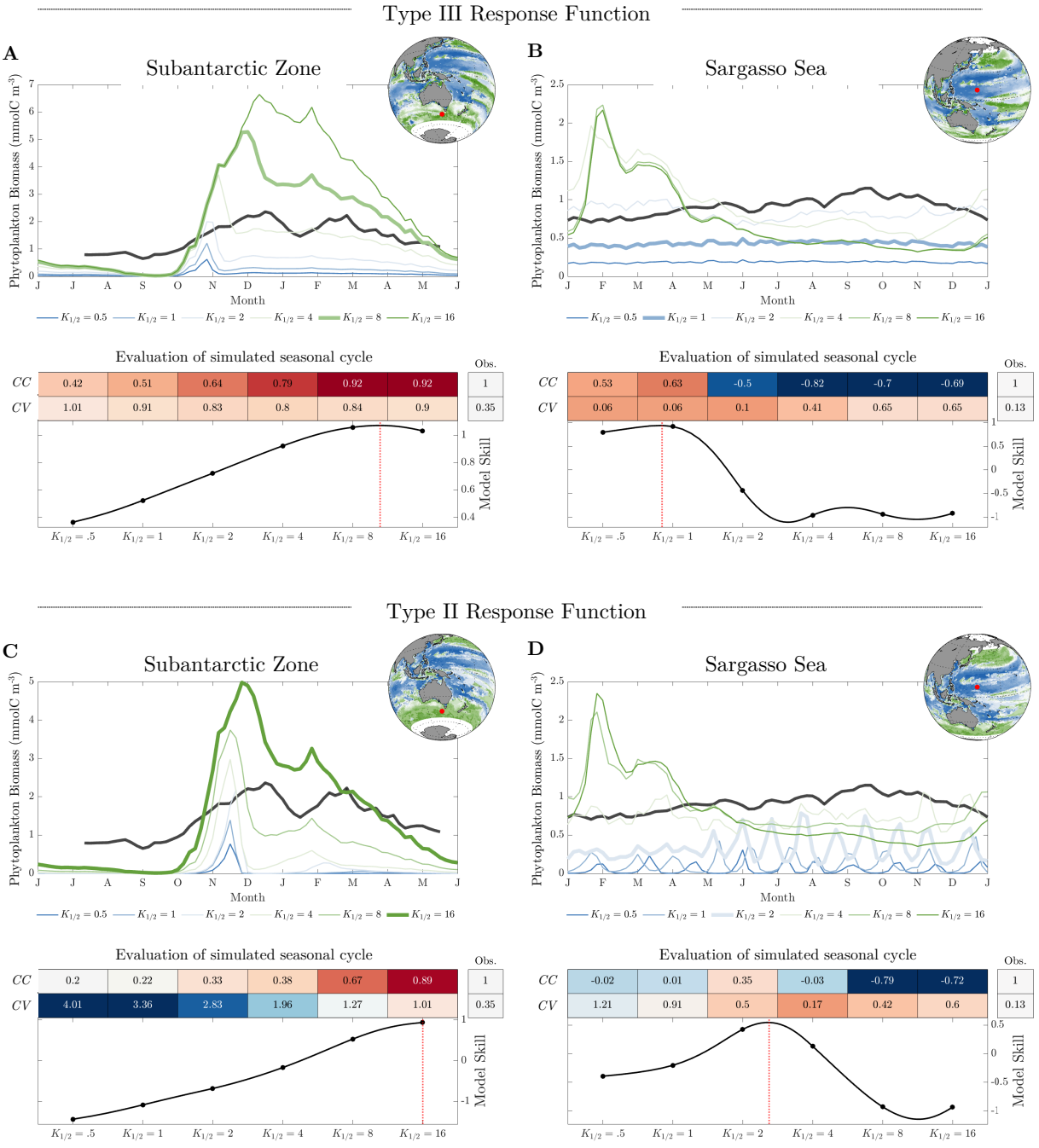

Figure 2. Influence of $K_{1/2}$ and response type on phytoplankton seasonal cycle. Phytoplankton biomass climatologies and model skill evaluations are provided from **A, C** the SAZ and **B, D** Sargasso Sea, showing the emergent seasonal cycle from runs using six $K_{1/2}$ values with a **A, B** Type III and **C, D** type II functional response. All simulations shown use identical g_{max} values (1 d^{-1}). In the upper panel of each subplot, the observed (black) and simulated (blue-green) seasonal cycles are plotted with the simulation that best matches the observed phenology in bold. In the lower panel, the cost function scoring is demonstrated for each simulation, with the corresponding CC and CV shown above the total cost function score. Red and blue shading indicates better and worse model skill, respectively. The optimal $K_{1/2}$ value is determined by the maximum (red line) interpolated model skill (black line). In the inset map (top-right corner) the distribution of optimal $K_{1/2}$ values is shown with the example location marked in red. Note, these distributions are qualitatively identical to Figure 1, with the same percentile-based colorbar. However, they only consider runs with $g_{max} = 1$ to be consistent with the traces, rather than the mean of all three g_{max} sets.

III response. The bloom is a sharper because lowering $K_{1/2}$ in a type II response destabilizes the system, allowing phytoplankton biomass to accumulate rapidly until bottom-up factors respond (i.e. nutrient limitation, self-shading) and rapidly terminate the bloom.

In the Sargasso Sea (**Figure 2B, D**), the observed evolution of biomass (black line) exhibits a weaker seasonal cycle, with an amplitude less than half the size of its mean. It is best recreated using smaller $K_{1/2}$ values and a type III response. With a type III response (**Figure 2B**), highly-stable lower $K_{1/2}$ values dampen seasonality in bottom-up controls and prevent a bloom. Increasing $K_{1/2}$ allows an unrealistic late-winter/early-spring bloom to emerge, systematically increasing the CV and decreasing model skill. While the emergent seasonal cycle is nearly identical between response curves when using high $K_{1/2}$ values (**Figure 2D**), the Type II response diverges substantially when using low $K_{1/2}$ values. Here, decreasing stability introduces unstable predator-prey dynamics which drive higher-frequency oscillations. Thus, the model cannot eliminate the unnatural early-spring bloom without inducing unnatural sub-seasonal spikes, neither of which are observed.

4 Discussion

4.1 Limitations

The largest limitation of these results likely stems from the accuracy of non-grazing attributes in the BGC-ocean model we have optimized. Despite running experiments in an identical physical ocean, if their is a systematic bias in the simulated seasonal light and nutrient cycle, then it is possible that the 'wrong' grazing dynamics could combine with the 'wrong' bottom-up controls to produce the correct seasonal cycle, leading us to infer unnatural grazing dynamics. This could be the case along the equator where there is a disproportionately large bias in phytoplankton biomass relative to NPP (**Supporting Figure 4**), suggesting simulated phytoplankton-specific growth rates are systematically low. This may explain why we inferred higher $K_{1/2}$ values in the equatorial Indian, Atlantic, and Pacific basins (**Figure 1B**; greener) than we would have expected from the low mean-annual phytoplankton biomass observed there (**Figure 1A**; bluer). If the model is misrepresenting the seasonal cycle in bottom-up controls as too weak, it makes sense that higher $K_{1/2}$ values are needed to not damp out all seasonal variability and recreate the observed seasonal cycle. Additional biases may stem from the remote sensing products, which are limited by clouds and the solar inclination angle, the exact nature of the link between trophic controls and bloom phenology (Behrenfeld et al., 2013; Rohr et al., 2017), and our ability to accurately quantify the fidelity of the seasonal cycle. Collectively then, our results our best understood qualitatively, rather than as specific quantitative predictions of the apparent $K_{1/2}$ value in any specific location.

4.2 Ecological Perspectives

Nevertheless, our inferred distribution of community-integrated grazing dynamics is consistent with the biogeography of community composition which we would expect to inhabit each respective biome (Barton et al., 2013; Heneghan et al., 2020; Décima, 2022; Brandão et al., 2021). Ecologically, the value of $K_{1/2}$ at a fixed g_{max} is related to the rate at which zooplankton can capture (rather than consume) prey (Rohr et al., 2022). Physiologically, the zooplankton with fastest prey capture rates are typically rapidly-grazing microzooplankton and filter feeders (Hansen et al., 1997). However, these zooplankton species are generally unable to consume anything larger than small flagellates, ciliates and cyanobacteria, exactly the sort of phytoplankton that tend to dominate more oligotrophic regions such as the gyres (Calbet & Landry, 2004). On the other hand, slowly-grazing euphausiids, copepods and macrozooplankton tend to have much slower capture rates but are capable of consuming much larger prey, such as dinoflagellates and diatom

assemblages, which tend to dominate more eutrophic coastal and higher-latitude regions (San Martin et al., 2006).

The sigmoidal relationship between phytoplankton biomass and inferred community-integrated $K_{1/2}$ values implies the importance of two end-member communities in the most oligotrophic and eutrophic regions. The location of each asymptotes implies a community integrated $K_{1/2}$ value of 3 mmolC m^{-3} for ecosystems dominated by faster-grazing microzooplankton and filter feeders and 8.3 mmolC m^{-3} for ecosystems dominated by slower-grazing mesozooplankton and macrozooplantkon. While these values are lower than the median empirical $K_{1/2}$ values measured by Hansen et al. (1997) in individual microzooplankton (8.9 mmolC m^{-3}) and mesozooplantkon (18 mmolC m^{-3}), the apparent $K_{1/2}$ of spatially-averaged, community-integrated dynamics is expected to be much lower than that of any individual species measured in well-mixed laboratory medium (Rohr et al., 2022).

However, despite two prominent asymptotes, the region of monotonically increasing $K_{1/2}$ values between them ($\sim$.85-1.2 mmolC m^{-3}) encompasses over 50% of the ocean area in our domain (55°S-55°N) and 43% of the global ocean. This suggests a critical role for more heterogeneous zooplankton communities and the co-existance of diverse functional groups therein. This steady increase in $K_{1/2}$ across intermediate mean-annual phytoplankton concentrations is consistent with the positive relationship between empirically estimated microzooplankton $K_{1/2}$ values and in-situ chlorophyll concentrations measured across shipboard dilution experiments (Chen et al., 2014). Note, while these results strongly imply slower zooplankton-specific grazing rates in more productive biomes, they can be consistent with observations of bulk ingestion rates and phytoplankton-specific grazing mortality increasing with primary productivity (Schmoker et al., 2013; Calbet, 2001) due to differences in phytoplankton and zooplankton abundance.

Finally, while community-integrated $K_{1/2}$ values exhibit large regional variability, the spatially integrated dynamics of all biomes are consistently best described by a type III versus type II response (Figure 1, Supporting Table 1). Although dynamic instabilities are not necessarily unnatural (McCauley & Murdoch, 1987), when averaged across a relatively large area the destabilizing properties of a type II response appear to lead to sharper, more delayed blooms than observed in eutrophic regions and more sub-seasonal variability than observed in eutrophic regions (Figure 2). This is consistent with observational (Morozov et al., 2008; Kiørboe, 2018), modelling (Nissen et al., 2018; Prowe et al., 2012; Chenillat et al., 2021), and theoretical (Rohr et al., 2022; Morozov, 2010) work suggesting that the downward concavity, prey refuge, and stabilizing properties associated with a type III response may be a better empirical representation of the mean state of a patchy ocean and complex food web, even if a type II response is typically measured for individual species in a well-mixed laboratory medium (Hansen et al., 1997; Hirst & Bunker, 2003).

4.3 Modelling Perspectives

Considering the sensitivity of simulated carbon cycling to the representation of zooplankton grazing dynamics (Rohr et al., 2023; Chenillat et al., 2021; Prowe et al., 2012; Laufkötter et al., 2015, 2016; Dupont et al., 2023), it is critical for models to accurately recreate the distribution community-integrated grazing dynamics and allow it to respond to environmental change. As warming, stratification, and stronger winds transform the surface ocean, the ensuing balance of light and nutrients may reshape marine ecosystems (Pörtner et al., 2019), favouring different zooplankton species, in different places, with vastly different grazing dynamics. For instance, a shift toward smaller phytoplankton, which have higher light but lower nutrient requirements (Pörtner et al., 2019; Bopp et al., 2005) would precipitate a shift towards microzooplankton, salps and larvaceans. Already a southward shift of salps into regions previously dominated by euphausiids has

been observed (Henschke & Pakhomov, 2019; Steinberg & Landry, 2017). Such shifts should be captured in BGC models if Earth system and ecosystem models hope to predict changes in the oceans capacity to buffer a changing climate and feed a growing population.

Fortunately, the validation of zooplankton biomass in BGC models is receiving increasing attention (Petrik et al., 2022; McGinty et al., 2023). However, given large uncertainties in the parameterization of grazing within ostensibly similar zooplankton functional groups across models (Rohr et al., 2022, 2023), a further validation of zooplankton-specific grazing rates is required to determine if a model is accurately simulating grazing pressure (i.e. the phytoplankton-specific mortality rate to grazing), which may be the single largest source of uncertainty in CMIP6 representations of marine carbon cycling (Rohr et al., 2023). While direct field measurements of grazing rates are typically limited to the role of microzooplankton (Schmoker et al., 2013; Calbet & Landry, 2004; Landry & Calbet, 2004) our results implicitly reflect the integrated grazing dynamics of the entire zooplankton community, averaging over the distribution and behavior of individual species.

First off, it appears clear that modellers should use a type III over type II response, especially if explicitly resolving a limited food web with relatively coarse spatial resolution. Further, although our exact quantitative estimates of $K_{1/2}$ are limited and vary with other model parameters (**Supporting Table 1**), there is a consistent qualitative pattern in apparent $K_{1/2}$ values which models ought to recreate. At minimum, it is clear a priori that models with a single zooplankton and prey option (e.g. Tjiputra et al. (2020); Zahariev et al. (2008); Law et al. (2017)) cannot simulate the established spatial variability in community-integrated grazing dynamics (as the single zooplankton will graze with the same $K_{1/2}$ everywhere). In turn, bottom-up controls are likely over-tuned to compensate for unrealistic top-down homogeneity. While many CMIP6-class models include 2-3 zooplankton groups (Kearney et al., 2021; Rohr et al., 2023), it is critical to know if competition between them is sufficient to drive a realistic emergent distribution in community-integrated grazing dynamics. Thus, we encourage modellers to confirm whether the distribution of community-integrated $K_{1/2}$ values is qualitatively consistent with **Figure 1**. This can be done by fitting a curve between the mean zooplankton-specific grazing rate and total prey concentration in different regions or grid cells to diagnostically compute the apparent functional response and associated community-integrated $K_{1/2}$ value. Significant disagreement from **Figure 1** would likely imply that additional zooplankton groups, such as macrozooplankton (Le Quéré et al., 2016), salps (Luo et al., 2020), larvaceans, euphausiids, chaetognaths, jellyfish (Heneghan et al., 2020, 2023) may be required.

Finally, if explicit competition between limited functional groups is insufficient to resolve the emergent distribution of community-integrated grazing dynamics and a sufficiently complex food web is not computationally tractable with high-resolution projections (Neelin et al., 2010), then modellers might consider parameterizing zooplankton community composition using the relationship described in **Figure 1**. That is, modellers could implicitly represent changes in zooplankton community composition by modifying $K_{1/2}$ of a single group as a function of phytoplankton abundance (**Supporting Table 1**). This could allow allow the mean attributes of the zooplankton community to respond dynamically to changing environmental conditions without explicitly resolving each of its constituent species. While potentially powerful, implementing such a parameterization would require several important assumptions and careful calibrations (**Supporting Text 3**).

5 Conclusions

These results present a novel, observationally-informed, map of global community-integrated grazing dynamics (i.e $K_{1/2}$ values). Further refining the observed distribu-

tion and drivers of grazing, and how to replicate them in models, will require close collaboration with zooplankton ecologists, but presents an exciting new frontier in oceanography focused on a rigorous understanding of how NPP is controlled from the top-down. Moreover, improving the representation of zooplankton could realize dramatic improvements in marine BGC models and our predictions of future ocean states.

6 Open Research

All relevant model output and documentation can be found at https://doi.org/10.25919/wn09-6j31. Remote sensing products were downloaded at `http://orca.science.oregonstate.edu/2160.by.4320.8day.hdf.carbon2.m.php`. Please address any questions to Tyler Rohr, at tyler.rohr@utas.edu.au.

Acknowledgments

This research was supported by the Australian Antarctic Program Partnership through the Australian Government's Antarctic Science Collaboration Initiative.

References

Adjou, M., Bendtsen, J., & Richardson, K. (2012, January). Modeling the influence from ocean transport, mixing and grazing on phytoplankton diversity. *Ecological Modelling*, *225*, 19–27. doi: 10.1016/j.ecolmodel.2011.11.005

Archibald, K. M., Siegel, D. A., & Doney, S. C. (2019). Modeling the Impact of Zooplankton Diel Vertical Migration on the Carbon Export Flux of the Biological Pump. *Global Biogeochemical Cycles*, *33*(2), 181–199. Retrieved 2022-02-03, from `https://onlinelibrary.wiley.com/doi/abs/10.1029/2018GB005983` doi: 10.1029/2018GB005983

Armengol, L., Calbet, A., Franchy, G., Rodríguez-Santos, A., & Hernández-León, S. (2019, February). Planktonic food web structure and trophic transfer efficiency along a productivity gradient in the tropical and subtropical Atlantic Ocean. *Scientific Reports*, *9*(1), 2044. (Publisher: Nature Publishing Group tex.copyright: 2019 The Author(s)) doi: 10.1038/s41598-019-38507-9

Barton, A. D., Pershing, A. J., Litchman, E., Record, N. R., Edwards, K. F., Finkel, Z. V., ... Ward, B. A. (2013). The biogeography of marine plankton traits. *Ecology Letters*, *16*(4), 522–534. Retrieved 2023-01-19, from `https://onlinelibrary.wiley.com/doi/abs/10.1111/ele.12063` doi: 10.1111/ele.12063

Behrenfeld, M. J., Doney, S. C., Lima, I., Boss, E. S., & Siegel, D. A. (2013). Annual cycles of ecological disturbance and recovery underlying the subarctic Atlantic spring plankton bloom. *Global Biogeochemical Cycles*, *27*(2), 526–540. Retrieved 2022-03-08, from `https://onlinelibrary.wiley.com/doi/abs/10.1002/gbc.20050` doi: 10.1002/gbc.20050

Bopp, L., Aumont, O., Cadule, P., Alvain, S., & Gehlen, M. (2005). Response of diatoms distribution to global warming and potential implications: A global model study. *Geophysical Research Letters*, *32*(19). Retrieved 2023-03-26, from `https://onlinelibrary.wiley.com/doi/abs/10.1029/2005GL023653` doi: 10.1029/2005GL023653

Brandão, M. C., Benedetti, F., Martini, S., Soviadan, Y. D., Irisson, J.-O., Romagnan, J.-B., ... Lombard, F. (2021, August). Macroscale patterns of oceanic zooplankton composition and size structure. *Scientific Reports*, *11*(1), 15714. Retrieved 2022-03-07, from `https://www.nature.com/articles/s41598-021-94615-5` doi: 10.1038/s41598-021-94615-5

Calbet, A. (2001). Mesozooplankton grazing effect on primary production: A global comparative analysis in marine ecosystems. *Limnology and*

Oceanography, *46*(7), 1824–1830. Retrieved 2023-02-20, from https://onlinelibrary.wiley.com/doi/abs/10.4319/lo.2001.46.7.1824 doi: 10.4319/lo.2001.46.7.1824

Calbet, A., & Landry, M. R. (2004). Phytoplankton growth, microzooplankton grazing, and carbon cycling in marine systems. *Limnology and Oceanography*, *49*(1), 51–57. Retrieved 2023-02-02, from https://onlinelibrary.wiley.com/doi/abs/10.4319/lo.2004.49.1.0051 doi: 10.4319/lo.2004.49.1.0051

Calbet, A., Martínez, R. A., Isari, S., Zervoudaki, S., Nejstgaard, J. C., Pitta, P., ... Ptacnik, R. (2012, August). Effects of light availability on mixotrophy and microzooplankton grazing in an oligotrophic plankton food web: Evidences from a mesocosm study in Eastern Mediterranean waters. *Journal of Experimental Marine Biology and Ecology*, *424-425*, 66–77. Retrieved 2023-02-20, from https://www.sciencedirect.com/science/article/pii/S0022098112001700 doi: 10.1016/j.jembe.2012.05.005

Calbet, A., Saiz, E., Almeda, R., Movilla, J. I., & Alcaraz, M. (2011, May). Low microzooplankton grazing rates in the Arctic Ocean during a Phaeocystis pouchetii bloom (Summer 2007): fact or artifact of the dilution technique? *Journal of Plankton Research*, *33*(5), 687–701. Retrieved 2023-02-20, from https://doi.org/10.1093/plankt/fbq142 doi: 10.1093/plankt/fbq142

Chen, B., Laws, E. A., Liu, H., & Huang, B. (2014). Estimating microzooplankton grazing half-saturation constants from dilution experiments with nonlinear feeding kinetics. *Limnology and Oceanography*, *59*(3), 639–644. doi: 10.4319/lo.2014.59.3.0639

Chenillat, F., Rivière, P., & Ohman, M. D. (2021, May). On the sensitivity of plankton ecosystem models to the formulation of zooplankton grazing. *PLOS ONE*, *16*(5), e0252033. Retrieved 2021-05-27, from https://journals.plos.org/plosone/article?id=10.1371/journal.pone.0252033 doi: 10.1371/journal.pone.0252033

de la Rocha, C. L. (2006). Chapter 5. The Biological Pump. In *The Oceans and Marine Geochemistry - 1st Edition* (1st Edition ed.). Pergamon.

Deppeler, S. L., & Davidson, A. T. (2017). Southern Ocean Phytoplankton in a Changing Climate. *Frontiers in Marine Science*, *4*. doi: 10.3389/fmars.2017.00040

Druon, J.-N., Hélaouët, P., Beaugrand, G., Fromentin, J.-M., Palialexis, A., & Hoepffner, N. (2019, March). Satellite-based indicator of zooplankton distribution for global monitoring. *Scientific Reports*, *9*(1), 4732. Retrieved 2023-01-19, from https://www.nature.com/articles/s41598-019-41212-2 doi: 10.1038/s41598-019-41212-2

Dunn, R. P., & Hovel, K. A. (2020, January). Predator type influences the frequency of functional responses to prey in marine habitats. *Biology Letters*, *16*(1), 20190758. (Publisher: Royal Society) doi: 10.1098/rsbl.2019.0758

Dupont, L., Le Mézo, P., Aumont, O., Bopp, L., Clerc, C., Ethé, C., & Maury, O. (2023). High trophic level feedbacks on global ocean carbon uptake and marine ecosystem dynamics under climate change. *Global Change Biology*, *29*(6). Retrieved 2023-01-08, from https://onlinelibrary.wiley.com/doi/abs/10.1111/gcb.16558 (https://onlinelibrary.wiley.com/doi/abs/10.1111/gcb.16558) doi: 10.1111/gcb.16558

Décima, M. (2022, June). Zooplankton trophic structure and ecosystem productivity. *Marine Ecology Progress Series*, *692*, 23–42. Retrieved 2023-05-04, from https://www.int-res.com/abstracts/meps/v692/p23-42/ doi: 10.3354/meps14077

Everett, J. D., Baird, M. E., Buchanan, P., Bulman, C., Davies, C., Downie, R., ... Richardson, A. J. (2017). Modeling What We Sample and Sampling What We Model: Challenges for Zooplankton Model Assessment. *Frontiers in Marine*

Science, *4*, 77. Retrieved 2021-10-19, from https://www.frontiersin.org/article/10.3389/fmars.2017.00077 doi: 10.3389/fmars.2017.00077

Fu, W., Randerson, J. T., & Moore, J. K. (2016, September). Climate change impacts on net primary production (NPP) and export production (EP) regulated by increasing stratification and phytoplankton community structure in the CMIP5 models. *Biogeosciences*, *13*(18), 5151–5170. Retrieved 2022-02-01, from https://bg.copernicus.org/articles/13/5151/2016/bg-13-5151-2016.html doi: 10.5194/bg-13-5151-2016

Gentleman, W. C., & Neuheimer, A. B. (2008, November). Functional responses and ecosystem dynamics: How clearance rates explain the influence of satiation, food-limitation and acclimation. *Journal of Plankton Research*, *30*(11), 1215–1231. doi: 10.1093/plankt/fbn078

Griffies, S. M. (2012). *Elements of MOM5, GFDL Ocean Group Technical Report No. 7* (Tech. Rep.). NOAA/Geophysical Fluid Dynamics Laboratory. Retrieved from https://mom-ocean.github.io/assets/pdfs/MOM5_manual.pdf

Guidi, L., Chaffron, S., Bittner, L., Eveillard, D., Larhlimi, A., Roux, S., ... Gorsky, G. (2016, April). Plankton networks driving carbon export in the oligotrophic ocean. *Nature*, *532*(7600), 465–470. doi: 10.1038/nature16942

Hansen, P. J., Bjørnsen, P. K., & Hansen, B. W. (1997). Zooplankton grazing and growth: Scaling within the 2-2,-Mm body size range. *Limnology and Oceanography*, *42*(4), 687–704. doi: 10.4319/lo.1997.42.4.0687

Hashioka, T., Vogt, M., Yamanaka, Y., Le Quéré, C., Buitenhuis, E. T., Aita, M. N., ... Doney, S. C. (2013, November). Phytoplankton competition during the spring bloom in four plankton functional type models. *Biogeosciences*, *10*(11), 6833–6850. Retrieved 2023-01-31, from https://bg.copernicus.org/articles/10/6833/2013/bg-10-6833-2013.html doi: 10.5194/bg-10-6833-2013

Heneghan, R. F., Everett, J. D., Blanchard, J. L., Sykes, P., & Richardson, A. J. (2023, March). Climate-driven zooplankton shifts cause large-scale declines in food quality for fish. *Nature Climate Change*, 1–8. Retrieved 2023-03-27, from https://www.nature.com/articles/s41558-023-01630-7 doi: 10.1038/s41558-023-01630-7

Heneghan, R. F., Everett, J. D., Sykes, P., Batten, S. D., Edwards, M., Takahashi, K., ... Richardson, A. J. (2020, November). A functional size-spectrum model of the global marine ecosystem that resolves zooplankton composition. *Ecological Modelling*, *435*, 109265. Retrieved 2021-08-10, from https://www.sciencedirect.com/science/article/pii/S0304380020303355 doi: 10.1016/j.ecolmodel.2020.109265

Henschke, N., & Pakhomov, E. A. (2019). Latitudinal variations in Salpa thompsoni reproductive fitness. *Limnology and Oceanography*, *64*(2), 575–584. Retrieved 2022-11-25, from https://onlinelibrary.wiley.com/doi/abs/10.1002/lno.11061 (_eprint: https://onlinelibrary.wiley.com/doi/pdf/10.1002/lno.11061) doi: 10.1002/lno.11061

Hernández-García, E., & López, C. (2004, September). Sustained plankton blooms under open chaotic flows. *Ecological Complexity*, *1*(3), 253–259. doi: 10.1016/j.ecocom.2004.05.002

Hirst, A. G., & Bunker, A. J. (2003). Growth of marine planktonic copepods: Global rates and patterns in relation to chlorophyll a, temperature, and body weight. *Limnology and Oceanography*, *48*(5), 1988–2010. doi: 10.4319/lo.2003.48.5.1988

Howarth, R. W. (1988, November). Nutrient limitation of net primary production in marine ecosystems. *Annual Review of Ecology and Systematics*, *19*(1), 89–110. (Publisher: Annual Reviews) doi: 10.1146/annurev.es.19.110188.000513

Kearney, K. A., Bograd, S. J., Drenkard, E., Gomez, F. A., Haltuch, M., Hermann,

A. J., ... Woodworth-Jefcoats, P. A. (2021). Using Global-Scale Earth System Models for Regional Fisheries Applications. *Frontiers in Marine Science*, *8*, 1121. Retrieved 2021-10-21, from https://www.frontiersin.org/article/10.3389/fmars.2021.622206 doi: 10.3389/fmars.2021.622206

Kiørboe, T. (2018). *A Mechanistic Approach to Plankton Ecology.* Princeton University Press. Retrieved 2023-01-31, from https://www.degruyter.com/document/doi/10.1515/9780691190310/html?lang=en doi: 10.1515/9780691190310

Kiørboe, T., & Hirst, A. G. (2014, April). Shifts in Mass Scaling of Respiration, Feeding, and Growth Rates across Life-Form Transitions in Marine Pelagic Organisms. *The American Naturalist*, *183*(4), E118–E130. Retrieved 2022-11-25, from https://www.journals.uchicago.edu/doi/10.1086/675241 (Publisher: The University of Chicago Press) doi: 10.1086/675241

Kwiatkowski, L., Torres, O., Bopp, L., Aumont, O., Chamberlain, M., Christian, J. R., ... Ziehn, T. (2020, July). Twenty-first century ocean warming, acidification, deoxygenation, and upper-ocean nutrient and primary production decline from CMIP6 model projections. *Biogeosciences*, *17*(13), 3439–3470. Retrieved 2022-03-19, from https://bg.copernicus.org/articles/17/3439/2020/ (Publisher: Copernicus GmbH) doi: 10.5194/bg-17-3439-2020

Landry, Ondrusek, M., Tanner, S., Brown, S., Constantinou, J., Bidigare, R., ... Fitzwater, S. (2000, August). Biological response to iron fertilization in the eastern equatorial Pacific (IronEx II). I. Microplankton community abundances and biomass. *Marine Ecology-progress Series - MAR ECOL-PROGR SER*, *201*, 27–42. doi: 10.3354/meps201027

Landry, M. R., Brown, S. L., Rii, Y. M., Selph, K. E., Bidigare, R. R., Yang, E. J., & Simmons, M. P. (2008, May). Depth-stratified phytoplankton dynamics in Cyclone Opal, a subtropical mesoscale eddy. *Deep Sea Research Part II: Topical Studies in Oceanography*, *55*(10), 1348–1359. Retrieved 2023-02-02, from https://www.sciencedirect.com/science/article/pii/S0967064508000921 doi: 10.1016/j.dsr2.2008.02.001

Landry, M. R., & Calbet, A. (2004, January). Microzooplankton production in the oceans. *ICES Journal of Marine Science*, *61*(4), 501–507. Retrieved 2023-03-26, from https://doi.org/10.1016/j.icesjms.2004.03.011 doi: 10.1016/j.icesjms.2004.03.011

Landry, M. R., Ohman, M. D., Goericke, R., Stukel, M. R., & Tsyrklevich, K. (2009, December). Lagrangian studies of phytoplankton growth and grazing relationships in a coastal upwelling ecosystem off Southern California. *Progress in Oceanography*, *83*(1), 208–216. Retrieved 2023-02-02, from https://www.sciencedirect.com/science/article/pii/S0079661109000846 doi: 10.1016/j.pocean.2009.07.026

Laufkötter, C., Vogt, M., Gruber, N., Aita-Noguchi, M., Aumont, O., Bopp, L., ... Völker, C. (2015, December). Drivers and Uncertainties of Future Global Marine Primary Production in Marine Ecosystem Models. *Biogeosciences*, *12*(23), 6955–6984. doi: 10.5194/bg-12-6955-2015

Laufkötter, C., Vogt, M., Gruber, N., Aumont, O., Bopp, L., Doney, S. C., ... Völker, C. (2016, July). Projected Decreases in Future Marine Export Production: The Role of the Carbon Flux through the Upper Ocean Ecosystem. *Biogeosciences*, *13*(13), 4023–4047. doi: 10.5194/bg-13-4023-2016

Law, R. M., Ziehn, T., Matear, R. J., Lenton, A., Chamberlain, M. A., Stevens, L. E., ... Vohralik, P. F. (2017, July). The carbon cycle in the Australian Community Climate and Earth System Simulator (ACCESS-ESM1) – Part 1: Model description and pre-industrial simulation. *Geoscientific Model Development*, *10*(7), 2567–2590. doi: 10.5194/gmd-10-2567-2017

Le Quéré, C., Buitenhuis, E. T., Moriarty, R., Alvain, S., Aumont, O., Bopp, L., ... Vallina, S. M. (2016, July). Role of Zooplankton Dynamics for Southern Ocean

Phytoplankton Biomass and Global Biogeochemical Cycles. *Biogeosciences*, *13*(14), 4111–4133. doi: 10.5194/bg-13-4111-2016

Lima-Mendez, G., Faust, K., Henry, N., Decelle, J., Colin, S., Carcillo, F., ... Raes, J. (2015, May). Determinants of community structure in the global plankton interactome. *Science*, *348*(6237). doi: 10.1126/science.1262073

Luo, J. Y., Condon, R. H., Stock, C. A., Duarte, C. M., Lucas, C. H., Pitt, K. A., & Cowen, R. K. (2020). Gelatinous Zooplankton-Mediated Carbon Flows in the Global Oceans: A Data-Driven Modeling Study. *Global Biogeochemical Cycles*, *34*(9), e2020GB006704. Retrieved 2022-07-20, from https://onlinelibrary.wiley.com/doi/abs/10.1029/2020GB006704 doi: 10.1029/2020GB006704

Malchow, H., Hilker, F. M., Sarkar, R. R., & Brauer, K. (2005, November). Spatiotemporal patterns in an excitable plankton system with lysogenic viral infection. *Mathematical and Computer Modelling*, *42*(9), 1035–1048. doi: 10.1016/j.mcm.2004.10.025

McCauley, E., & Murdoch, W. W. (1987, January). Cyclic and Stable Populations: Plankton as Paradigm. *The American Naturalist*, *129*(1), 97–121. Retrieved 2021-08-20, from https://www.journals.uchicago.edu/doi/abs/10.1086/284624 (Publisher: The University of Chicago Press) doi: 10.1086/284624

McGinty, N., Irwin, A. J., Finkel, Z. V., & Dutkiewicz, S. (2023). Using ecological partitions to assess zooplankton biogeography and seasonality. *Frontiers in Marine Science*, *10*. Retrieved 2023-05-04, from https://www.frontiersin.org/articles/10.3389/fmars.2023.989770

Mojica, K., Behrenfeld, M., Clay, M., & Brussaard, C. (2021, August). Spring Accumulation Rates in North Atlantic Phytoplankton Communities Linked to Alterations in the Balance Between Division and Loss. *Frontiers in Microbiology*, *12*. doi: 10.3389/fmicb.2021.706137

Morozov, A. (2010). Emergence of Holling type III zooplankton functional response: Bringing together field evidence and mathematical modelling. *Journal of Theoretical Biology*, *265*(1), 45–54. doi: 10.1016/j.jtbi.2010.04.016

Morozov, A., & Arashkevich, E. (2010, January). Towards a correct description of zooplankton feeding in models: Taking into account food-mediated unsynchronized vertical migration. *Journal of Theoretical Biology*, *262*(2), 346–360. Retrieved 2022-04-21, from https://www.sciencedirect.com/science/article/pii/S0022519309004536 doi: 10.1016/j.jtbi.2009.09.023

Morozov, A., Arashkevich, E., Reigstad, M., & Falk-Petersen, S. (2008, October). Influence of spatial heterogeneity on the type of zooplankton functional response: A study based on field observations. *Deep Sea Research Part II: Topical Studies in Oceanography*, *55*(20), 2285–2291. doi: https://doi.org/10.1016/j.dsr2.2008.05.008

Morrow, R. M., Ohman, M. D., Goericke, R., Kelly, T. B., Stephens, B. M., & Stukel, M. R. (2018, October). CCE V: Primary production, mesozooplankton grazing, and the biological pump in the California Current Ecosystem: Variability and response to El Niño. *Deep Sea Research Part I: Oceanographic Research Papers*, *140*, 52–62. Retrieved 2023-02-02, from https://www.sciencedirect.com/science/article/pii/S096706371830013X doi: 10.1016/j.dsr.2018.07.012

Mortenson, E., Lenton, A., Shadwick, E. H., Trull, T. W., Chamberlain, M. A., & Zhang, X. (2021, December). Divergent trajectories of ocean warming and acidification. *Environmental Research Letters*, *16*(12), 124063. Retrieved 2022-03-19, from https://doi.org/10.1088/1748-9326/ac3d57 doi: 10.1088/1748-9326/ac3d57

Neelin, J. D., Bracco, A., Luo, H., McWilliams, J. C., & Meyerson, J. E. (2010, December). Considerations for parameter optimization and sensitivity in climate models. *Proceedings of the National Academy of Sciences*, *107*(50), 21349–

21354. Retrieved 2021-10-13, from https://www.pnas.org/content/107/50/21349 (Publisher: National Academy of Sciences Section: Physical Sciences) doi: 10.1073/pnas.1015473107

Nissen, C., Vogt, M., Münnich, M., Gruber, N., & Haumann, F. A. (2018, November). Factors controlling coccolithophore biogeography in the Southern Ocean. *Biogeosciences*, *15*(22), 6997–7024. Retrieved 2023-03-26, from https://bg.copernicus.org/articles/15/6997/2018/ doi: 10.5194/bg-15-6997-2018

Oke, P. R., Griffin, D. A., Schiller, A., Matear, R. J., Fiedler, R., Mansbridge, J., ... Ridgway, K. (2013, May). Evaluation of a near-global eddy-resolving ocean model. *Geoscientific Model Development*, *6*, 591–615. doi: 10.5194/gmd-6-591-2013

Petrik, C. M., Luo, J. Y., Heneghan, R. F., Everett, J. D., Harrison, C. S., & Richardson, A. J. (2022). Assessment and Constraint of Mesozooplankton in CMIP6 Earth System Models. *Global Biogeochemical Cycles*, *36*(11), e2022GB007367. doi: 10.1029/2022GB007367

Prowe, A. E. F., Pahlow, M., Dutkiewicz, S., Follows, M., & Oschlies, A. (2012, August). Top-down control of marine phytoplankton diversity in a global ecosystem model. *Progress in Oceanography*, *101*(1), 1–13. doi: 10.1016/j.pocean.2011.11.016

Pörtner, H., Roberts, D., Masson-Delmotte, V., Zhai, P., Tignor, M., Poloczanska, E., ... Weyer, N. (2019). *IPCC Special Report on the Ocean and Cryosphere in a Changing Climate* (Tech. Rep.). IPCC.

Ratnarajah, L., Abu-Alhaija, R., Atkinson, A., Batten, S., Bax, N. J., Bernard, K. S., ... Yebra, L. (2023, February). Monitoring and modelling marine zooplankton in a changing climate. *Nature Communications*, *14*(1), 564. Retrieved 2023-03-08, from https://www.nature.com/articles/s41467-023-36241-5 doi: 10.1038/s41467-023-36241-5

Richardson, A. J. (2008, April). In hot water: zooplankton and climate change. *ICES Journal of Marine Science*, *65*(3), 279–295. Retrieved 2021-10-19, from https://doi.org/10.1093/icesjms/fsn028 doi: 10.1093/icesjms/fsn028

Rohr, T., Long, M., T. Kavanaugh, M., Lindsay, K., & Doney, S. (2017, May). Variability in the Mechanisms Controlling Southern Ocean Phytoplankton Bloom Phenology in an Ocean Model and Satellite Observations. *Global Biogeochemical Cycles*, *31*. doi: 10.1002/2016gb005615

Rohr, T., Richardson, A., Lenton, A., Chamberlain, M., & Shadwick, E. (2023). Zooplankton grazing is the largest source of 1 uncertainty for marine carbon cycling in CMIP6 IPCC 2 models. *Communications Earth and Environment*, *Under Review - See 'Related Manuscript'*.

Rohr, T., Richardson, A. J., Lenton, A., & Shadwick, E. (2022, November). Recommendations for the formulation of grazing in marine biogeochemical and ecosystem models. *Progress in Oceanography*, *208*, 102878. Retrieved 2023-04-24, from https://www.sciencedirect.com/science/article/pii/S0079661122001379 doi: 10.1016/j.pocean.2022.102878

Roy, S., Sathyendranath, S., Bouman, H., & Platt, T. (2013, December). The global distribution of phytoplankton size spectrum and size classes from their light-absorption spectra derived from satellite data. *Remote Sensing of Environment*, *139*, 185–197. Retrieved 2022-11-25, from https://www.sciencedirect.com/science/article/pii/S0034425713002629 doi: 10.1016/j.rse.2013.08.004

San Martin, E., Harris, R. P., & Irigoien, X. (2006, July). Latitudinal variation in plankton size spectra in the Atlantic Ocean. *Deep Sea Research Part II: Topical Studies in Oceanography*, *53*(14), 1560–1572. Retrieved 2023-04-25, from https://www.sciencedirect.com/science/article/pii/S096706450600124X doi: 10.1016/j.dsr2.2006.05.006

Sathyendranath, S., Brewin, R. J. W., Brockmann, C., Brotas, V., Calton, B., Chuprin, A., ... Platt, T. (2019, January). An Ocean-Colour Time Series for Use in Climate Studies: The Experience of the Ocean-Colour Climate Change Initiative (OC-CCI). *Sensors*, *19*(19), 4285. doi: 10.3390/s19194285

Schmoker, C., Hernández-León, S., & Calbet, A. (2013, July). Microzooplankton grazing in the oceans: impacts, data variability, knowledge gaps and future directions. *Journal of Plankton Research*, *35*(4), 691–706. Retrieved 2023-02-02, from https://doi.org/10.1093/plankt/fbt023 doi: 10.1093/plankt/fbt023

Steele, J. (1974). Stability of plankton ecosystems. In M. B. Usher & M. H. Williamson (Eds.), *Ecological Stability* (pp. 179–191). Boston, MA: Springer US. doi: 10.1007/978-1-4899-6938-5_12

Steinberg, D. K., & Landry, M. R. (2017). Zooplankton and the Ocean Carbon Cycle. *Annual Review of Marine Science*, *9*(1), 413–444. Retrieved 2022-03-07, from https://doi.org/10.1146/annurev-marine-010814-015924 doi: 10.1146/annurev-marine-010814-015924

Steinberg, D. K., Ruck, K. E., Gleiber, M. R., Garzio, L. M., Cope, J. S., Bernard, K. S., ... Ross, R. M. (2015, July). Long-term (1993–2013) changes in macrozooplankton off the Western Antarctic Peninsula. *Deep Sea Research Part I: Oceanographic Research Papers*, *101*, 54–70. Retrieved 2021-11-25, from https://www.sciencedirect.com/science/article/pii/S0967063715000412 doi: 10.1016/j.dsr.2015.02.009

Strömberg, K. H. P., Smyth, T. J., Allen, J. I., Pitois, S., & O'Brien, T. D. (2009, August). Estimation of global zooplankton biomass from satellite ocean colour. *Journal of Marine Systems*, *78*(1), 18–27. Retrieved 2023-01-19, from https://www.sciencedirect.com/science/article/pii/S0924796309000669 doi: 10.1016/j.jmarsys.2009.02.004

Sverdrup, H. U. (1953, January). On Conditions for the Vernal Blooming of Phytoplankton. *ICES Journal of Marine Science*, *18*(3), 287–295. doi: 10.1093/icesjms/18.3.287

Tagliabue, A., Kwiatkowski, L., Bopp, L., Butenschön, M., Cheung, W., Lengaigne, M., & Vialard, J. (2021). Persistent Uncertainties in Ocean Net Primary Production Climate Change Projections at Regional Scales Raise Challenges for Assessing Impacts on Ecosystem Services. *Frontiers in Climate*, *3*. Retrieved 2022-02-07, from https://www.frontiersin.org/article/10.3389/fclim.2021.738224

Tittensor, D. P., Novaglio, C., Harrison, C. S., Heneghan, R. F., Barrier, N., Bianchi, D., ... Blanchard, J. L. (2021, October). Next-generation ensemble projections reveal higher climate risks for marine ecosystems. *Nature Climate Change*, 1–9. Retrieved 2021-10-25, from https://www.nature.com/articles/s41558-021-01173-9 doi: 10.1038/s41558-021-01173-9

Tjiputra, J. F., Schwinger, J., Bentsen, M., Morée, A. L., Gao, S., Bethke, I., ... Schulz, M. (2020, May). Ocean biogeochemistry in the Norwegian Earth System Model version 2 (NorESM2). *Geoscientific Model Development*, *13*(5), 2393–2431. Retrieved 2022-03-08, from https://gmd.copernicus.org/articles/13/2393/2020/ doi: 10.5194/gmd-13-2393-2020

Truscott, J. E., Brindley, J., Brindley, J., & Gray, P. (1994, June). Equilibria, stability and excitability in a general class of plankton population models. *Philosophical Transactions of the Royal Society of London. Series A: Physical and Engineering Sciences*, *347*(1685), 703–718. (Publisher: Royal Society) doi: 10.1098/rsta.1994.0076

Tsujino, H., Urakawa, S., Nakano, H., Small, R. J., Kim, W. M., Yeager, S. G., ... Yamazaki, D. (2020). input4MIPs.CMIP6.OMIP.MRI.MRI-JRA55-do-1-5-0. Retrieved 2022-03-19, from https://doi.org/10.22033/ESGF/input4MIPs.15017 (Publisher: Earth System Grid Federation Type: dataset)

790 doi: 10.22033/ESGF/input4MIPs.15017
791 Vallina, S. M., & Le Quéré, C. (2011, March). Stability of complex food webs:
792 Resilience, resistance and the average interaction strength. *Journal of The-*
793 *oretical Biology*, *272*(1), 160–173. Retrieved 2023-01-23, from `https://`
794 `www.sciencedirect.com/science/article/pii/S0022519310006387` doi:
795 10.1016/j.jtbi.2010.11.043
796 Vallina, S. M., Ward, B. A., Dutkiewicz, S., & Follows, M. J. (2014, January).
797 Maximal feeding with active prey-switching: A kill-the-winner functional
798 response and its effect on global diversity and biogeography. *Progress*
799 *in Oceanography*, *120*, 93–109. Retrieved 2023-01-17, from `https://`
800 `www.sciencedirect.com/science/article/pii/S0079661113001468` doi:
801 10.1016/j.pocean.2013.08.001
802 Westberry, T. K., Behrenfeld, M. J., Siegel, D. A., & Boss, E. S. (2008, June).
803 Carbon-Based Primary Productivity Modeling with Vertically Resolved
804 Photoacclimation. *Global Biogeochemical Cycles*, *22*(2). doi: 10.1029/
805 2007GB003078
806 Zahariev, K., Christian, J. R., & Denman, K. L. (2008, April). Preindustrial, Histor-
807 ical, and Fertilization Simulations Using a Global Ocean Carbon Model with
808 New Parameterizations of Iron Limitation, Calcification, and N 2 Fixation.
809 *Progress in Oceanography*, *77*, 56–82. doi: 10.1016/j.pocean.2008.01.007
810 Ziehn, T., Chamberlain, M. A., Law, R. M., Lenton, A., Bodman, R. W., Dix, M.,
811 ... Srbinovsky, J. (2020, August). The Australian Earth System Model:
812 ACCESS-ESM1.5. *Journal of Southern Hemisphere Earth Systems Science*,
813 *70*(1), 193–214. Retrieved 2021-05-27, from `https://www.publish.csiro.au/`
814 `es/ES19035` doi: 10.1071/ES19035
815 Ziehn, T., Lenton, A., Law, R., Matear, R., & Chamberlain, M. (2017, July). The
816 carbon cycle in the Australian Community Climate and Earth System Simu-
817 lator (ACCESS-ESM1) – Part 2: Historical simulations. *Geoscientific Model*
818 *Development*, *10*, 2591–2614. doi: 10.5194/gmd-10-2591-2017